

# Light-front quark model predictions of meson elastic and transition form factors

Chueng-Ryong Ji and Ho-Meoyng Choi

*Department of Physics, North Carolina State University, Raleigh,  
NC 27695-8202, USA*

*E-mail: ji@ncsu.edu*

We investigate the electroweak form factors and semileptonic decay rates of mesons using the constituent quark model based on the light-front degrees of freedom. Our results demonstrate the broader applicability of light-front approach including the timelike region of exclusive processes.

## 1 Introduction

One of the distinctive advantages in the light-front approach is the well-established formulation of various form factor calculations using the well-known Drell-Yan-West ( $q^+ = 0$ ) frame<sup>1</sup>. In  $q^+ = 0$  frame, only parton-number-conserving Fock state (valence) contribution is needed when the “good” components of the current,  $J^+$  and  $J_\perp = (J_x, J_y)$ , are used<sup>2</sup>. For example, only the valence diagram shown in Fig. 1(a) is used in the light-front quark model (LFQM) analysis of spacelike meson form factors. Successful LFQM description of various hadron form factors can be found in the literatures<sup>3,4,5</sup>.

However, the timelike ( $q^2 > 0$ ) form factor analysis in the LFQM has been hindered by the fact that  $q^+ = 0$  frame is defined only in the spacelike region ( $q^2 = q^+q^- - q_\perp^2 < 0$ ). While the  $q^+ \neq 0$  frame can be used in principle to compute the timelike form factors, it is inevitable (if  $q^+ \neq 0$ ) to encounter the nonvalence diagram arising from the quark-antiquark pair creation (so called “Z-graph”). For example, the nonvalence diagram in the case of semileptonic meson decays is shown in Fig. 1(b). The main source of the difficulty, however, in calculating the nonvalence diagram (see Fig. 1(b)) is the lack of information on the black blob which should contrast with the white blob representing the usual light-front valence wave function. In fact, we noticed<sup>2</sup> that the omission of nonvalence contribution leads to a large deviation from the full results. The timelike form factors associated with the hadron pair productions in  $e^+e^-$  annihilations also involve the nonvalence contributions. Therefore, it would be very useful to avoid encountering the nonvalence diagram and still be able to generate the results of timelike form factors.

In this paper, we start from the heuristic model calculations to obtain the exact result of the timelike form factor and then discuss our light-front constituent quark model predictions for the meson electroweak form factors.

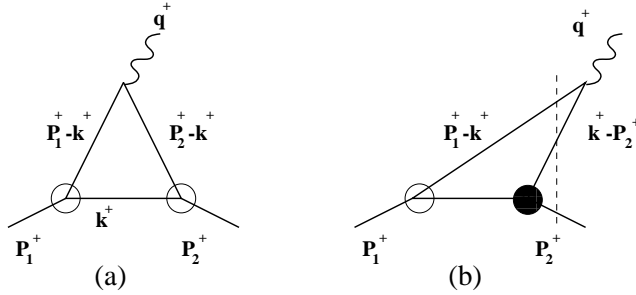


Figure 1: The LFQM description of a electroweak meson form factor: (a) the usual light-front valence diagram and (b) the nonvalence(pair-creation) diagram. The vertical dashed line in (b) indicates the energy-denominator for the nonvalence contributions. While the white blob represents the usual light-front valence wave function, the modeling of black blob has not yet been made.

Especially, we focus on the calculations of observables in timelike  $|Q^2|$  region overcoming the difficulties associated with the quark-antiquark pair creation in the light-front approach. As an explicit example of application to timelike  $|Q^2|$  region, we present our recent analysis of semileptonic weak decay processes. In Section 2, we present the heuristic model calculations to analytically continue the form factors in the spacelike region to those in the timelike region. In Section 3, we present our model calculations of semileptonic pseudoscalar meson decay processes as an example of application to the timelike  $|Q^2|$  region. Conclusions and discussions follow in Section 4.

## 2 Heuristic Model Calculations

Using the solution of covariant Bethe-Salpeter equation in the ladder approximation with a relativistic version of the contact interaction<sup>6</sup>, we can learn some lessons on the analytic continuation from the spacelike region to the timelike region<sup>7</sup>. The covariant model wave function is a product of two free single particle propagators, the overall momentum-conservation Dirac delta and a constant vertex function. Thus, all our form factor calculations in this section are nothing but various ways of evaluating the Feynman perturbation theory triangle diagram in scalar field theory<sup>7</sup>.

Using this model, we show an explicit example of generating the exact result of the timelike form factor without encountering the nonvalence diagram. This can be done by the analytic continuation from the spacelike form factor calculated in the Drell-Yan-West ( $q^+ = 0$ ) frame to the timelike region. To explicitly show it, we calculated<sup>7</sup>: (A) the timelike process of  $\gamma^* \rightarrow M + \bar{M}$

transition in  $q^+ \neq 0$  ( $q^2 > 0$ ) frame, (B) the spacelike process of  $M \rightarrow \gamma^* + M$  in  $q^+ \neq 0$  ( $q^2 < 0$ ) frame, and (C) the spacelike process of  $M \rightarrow \gamma^* + M$  in  $q^+ = 0$  frame. The analytic continuation from  $q^2 < 0$  to  $q^2 > 0$  allows us to show that the result in (C), which is obtained without encountering the nonvalence contributions at all, exactly reproduces the result in (A). In fact, all three results (A), (B), and (C) coincide with each other in the entire  $q^2$  range. We also confirm that our results are consistent with the dispersion relations<sup>8</sup>. We consider here only for the equal quark/antiquark mass case such as the pion. However, the unequal mass cases such as  $K$  and  $D$  were also shown in Ref.[7].

For our numerical analysis of  $\pi$  meson form factor, we use the following constituent quark and antiquark masses:  $m_u = m_d = 0.25$  GeV. Since our numerical results of the EM form factors obtained from (A), (B), and (C) turn out to be exactly same with each other for the entire  $q^2$  region, each line depicted in Figs. 2 and 3 represents all three results.

As a consistency check, we also compare our numerical results of the form factor  $F(q^2) = \text{Re } F(q^2) + i \text{Im } F(q^2)$  with the dispersion relations given by

$$\text{Re } F(q^2) = \frac{1}{\pi} P \int_{-\infty}^{\infty} \frac{\text{Im } F(q'^2)}{q'^2 - q^2} dq'^2, \quad (1)$$

$$\text{Im } F(q^2) = -\frac{1}{\pi} P \int_{-\infty}^{\infty} \frac{\text{Re } F(q'^2)}{q'^2 - q^2} dq'^2, \quad (2)$$

where  $P$  indicates the Cauchy principal value.

In Fig. 2, we show the EM form factor of the pion for  $-2 \text{ GeV}^2 \leq q^2 \leq 3 \text{ GeV}^2$ . The imaginary part (the dotted line) of the form factor starts at  $q_{\text{min}}^2 = 4m_{u(d)}^2 = 0.25 \text{ GeV}^2$ . It is interesting to note that the square of the total form factor  $|F_\pi(q^2)|^2$  (thick solid line) produces a  $\rho$  meson-type peak near  $q^2 \sim M_\rho^2$ . However, it is not yet clear if this model indeed reproduces all the features of the vector meson dominance (VMD) phenomena. Even though the generated position of peak is consistent with VMD, the final state interaction is not included in this simple model calculation. We believe that much more complex mechanisms may be necessary to reproduce the realistic VMD phenomena. More detailed analysis along this line is under consideration. Nevertheless, it is remarkable that this simple model is capable of generating the peak and the position of peak is quite consistent with the VMD.

In Fig. 3, we show the timelike form factor of the pion for the entire  $q^2 > 0$  region and compare the imaginary part of our direct calculations (dotted line) obtained from (A), (B), and (C) with the result (data of black dots) obtained from the dispersion relations given by Eq. (2). Our direct calculation is in an

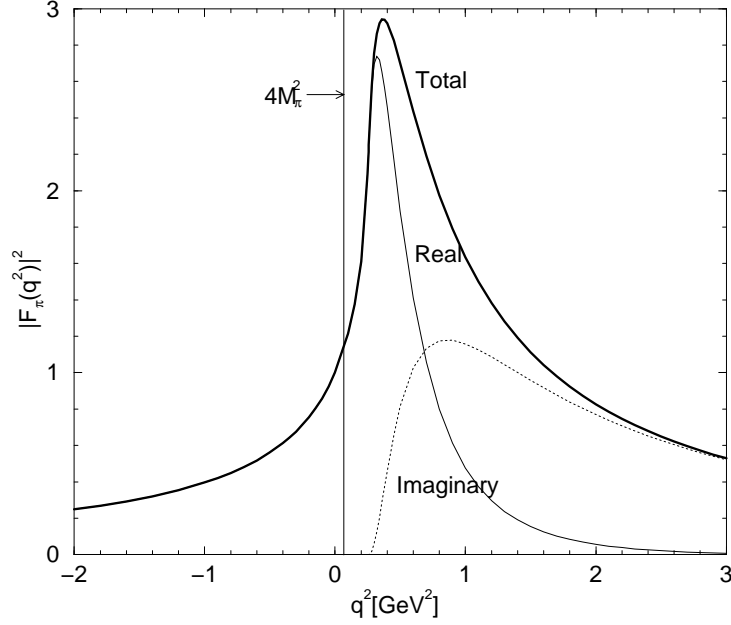


Figure 2: The electromagnetic form factor of the pion in (3+1) dimensional scalar field theory for  $-2 \leq q^2 \leq 3 \text{ GeV}^2$ . The total, real, and imaginary parts of  $|F_\pi(q^2)|^2$  are represented by thick solid, solid, and dotted lines, respectively.

excellent agreement with the solution of the dispersion relations. Our result for the real part are also confirmed to be in complete agreement with the dispersion relations. For high  $q^2$  region, the imaginary part of the form factor is dominant over the real part (thin solid line).

In Figs. 2 and 3, it is astonishing that the numerical result of (C) obtained from  $q^+ = 0$  frame without encountering the nonvalence diagram coincides exactly with the numerical results of (A) and (B) obtained from  $q^+ \neq 0$  frame.

### 3 Semileptonic Pseudoscalar Meson Decays in LFQM

The key idea in our LFQM<sup>5</sup> for mesons is to treat the radial wave function as a trial function for the variational principle to the QCD-motivated Hamiltonian

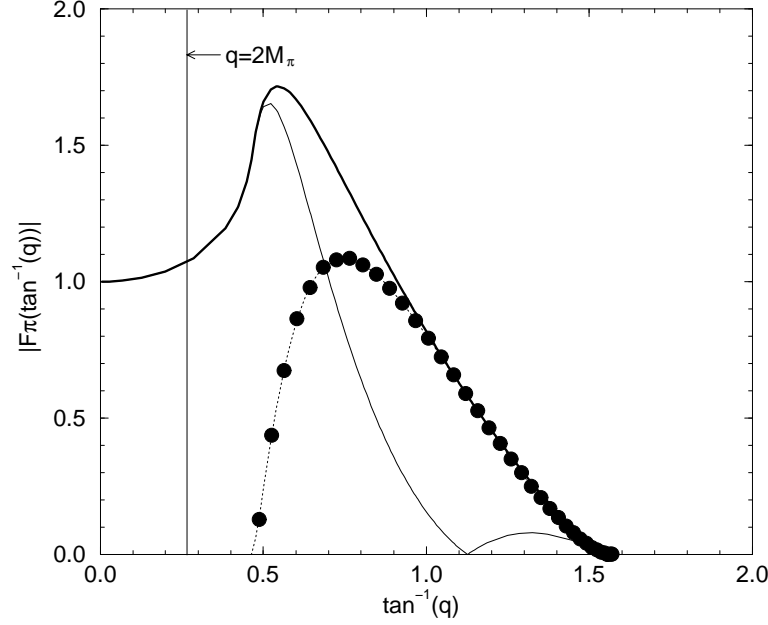


Figure 3: The electromagnetic form factor of the pion in (3 + 1) dimensional scalar field theory for the entire timelike region compared to the dispersion relations (data of black dots) given by Eq. (2). The same line code as in Fig. 2 is used.

saturation of the Fock state expansion by the constituent quark and antiquark. The spin-orbit wave function is uniquely determined by the Melosh transformation. We take the QCD-motivated effective Hamiltonian as the well-known linear plus Coulomb interaction given by

$$H_{q\bar{q}} = H_0 + V_{q\bar{q}} = \sqrt{m_q^2 + k^2} + \sqrt{m_{\bar{q}}^2 + k^2} + V_{q\bar{q}}, \quad (3)$$

where

$$V_{q\bar{q}} = V_0 + V_{\text{hyp}} = a + br - \frac{4\kappa}{3r} + \frac{2\vec{S}_q \cdot \vec{S}_{\bar{q}}}{3m_q m_{\bar{q}}} \nabla^2 V_{\text{Coul}}. \quad (4)$$

We take the Gaussian radial wave function  $\phi(k^2) = N \exp(-k^2/2\beta^2)$  as our trial wave function to minimize the central Hamiltonian<sup>5</sup>. Since the string

tension  $b=0.18 \text{ GeV}^2$  and the constituent  $u$  and  $d$  quark masses  $m_u=m_d=0.22 \text{ GeV}$  are rather well known from other quark model analyses commensurate with Regge phenomenology<sup>9</sup>, we take them as our input parameters. The model parameters of  $a, \kappa$ , and  $\beta_{u\bar{d}}$  are determined by the variational principle using the masses of  $\rho$  and  $\pi$ <sup>5,10</sup>. It is very important to note that all other model parameters such as  $m_c, m_b, \beta_{uc}, \beta_{ub}$ , etc. are then uniquely determined by our variational principle as shown in Ref.[10].

The semileptonic decays of a pseudoscalar meson  $Q_1\bar{q}$  into another pseudoscalar meson  $Q_2\bar{q}$  are governed by the weak vector current as follows

$$\langle P_2 | \bar{Q}_2 \gamma^\mu Q_1 | P_1 \rangle = f_+(q^2)(P_1 + P_2)^\mu + f_-(q^2)(P_1 - P_2)^\mu, \quad (5)$$

where  $q^\mu = (P_1 - P_2)^\mu$  is the four-momentum transfer to the leptons. In the LFQM calculations presented in Ref.[11], the  $q^+ \neq 0$  frame has been used to calculate the weak decays in the timelike region  $m_l^2 \leq q^2 \leq (M_1 - M_2)^2$ , with  $M_{1[2]}$  and  $m_l$  being the initial[final] meson mass and the lepton( $l$ ) mass, respectively. However, when the  $q^+ \neq 0$  frame is used, the inclusion of the non-valence contributions arising from quark-antiquark pair creation (“Z-graph”) is inevitable and this inclusion may be very important for heavy-to-light and light-to-light decays. Nevertheless, the previous analyses<sup>11</sup> in  $q^+ \neq 0$  frame considered only valence contributions neglecting nonvalence contributions. In this work, we circumvent this problem by calculating the processes in  $q^+ = 0$  frame and analytically continuing to the timelike region. The  $q^+ = 0$  frame is useful because only valence contributions are needed. However, one needs to calculate the component of the current other than  $J^+$  to obtain the form factor  $f_-(q^2)$ . Since  $J^-$  is not free from the zero-mode contributions even in  $q^+ = 0$  frame<sup>12</sup>, we use  $J_\perp$  instead of  $J^-$  to obtain  $f_-$ . In the  $q^+ = 0$  frame, we obtain the form factors  $f_+(q^2)$  and  $f_-(q^2)$  using the matrix element of the “+” and “ $\perp$ ”-components of the current,  $J^\mu$ , respectively, and then analytically continued to the timelike  $q^2 > 0$  region by changing  $q_\perp$  to  $iq_\perp$  in the form factors. Our numerical results of the decay rates for  $D \rightarrow \pi(K)$ ,  $D_s \rightarrow \eta(\eta')$ , and  $B \rightarrow \pi(D)$  processes are consistent with the experimental data as summarized in Table 1. It is interesting to note that our value of  $\eta$ - $\eta'$  mixing angle,  $\theta_{SU(3)} = -19^\circ$  presented in Ref.[5], are also in agreement with the data<sup>13</sup> for  $D_s \rightarrow \eta(\eta')$  decays. More detailed results are given in Ref.[10].

## 4 Conclusions and Discussions

Using the heuristic model presented in Section 2, we discussed the important issue in the light-front approach, i.e., the calculation of the timelike form factors. Even though the model was simple, it played the role of guidance for the

Table 1: Form factors  $f_+(0)$  and branching ratios (Br.) for various heavy meson semileptonic decays for  $0^- \rightarrow 0^-$ . We use  $\theta_{SU(3)}^{\eta-\eta'} = -19^\circ$  for  $D_s \rightarrow \eta(\eta')$  decays and the following CKM matrix element:  $|V_{cs}|=1.04 \pm 0.16$ ,  $|V_{cd}|=0.224 \pm 0.016$ ,  $|V_{ub}|=(3.3 \pm 0.4 \pm 0.7) \times 10^{-3}$ , and  $|V_{bc}|=0.0395 \pm 0.003$  [13].

Processes	$f_+(0)$	Br.	Expt. <sup>13</sup>
$D \rightarrow K$	0.736	$(3.75 \pm 1.16)\%$	$(3.66 \pm 0.18)\%$
$D \rightarrow \pi$	0.618	$(2.36 \pm 0.34) \times 10^{-3}$	$(3.9^{+2.3}_{-1.1} \pm 0.4) \times 10^{-3}$
$D_s \rightarrow \eta$	0.421	$(1.8 \pm 0.6)\%$	$(2.5 \pm 0.7)\%$
$D_s \rightarrow \eta'$	0.585	$(9.3 \pm 2.9) \times 10^{-3}$	$(8.8 \pm 3.4) \times 10^{-3}$
$B \rightarrow \pi$	0.273	$(1.40 \pm 0.34) \times 10^{-4}$	$(1.8 \pm 0.6) \times 10^{-4}$
$B \rightarrow D$	0.709	$(2.28 \pm 0.20)\%$	$(2.00 \pm 0.25)\%$

more realistic model calculation. Since this solvable model provides the full information for the nonvalence diagram (black blob in Fig. 1(b)), we were able to check if the analytic continuation of the result in the Drell-Yan-West ( $q^+ = 0$ ) frame (without the black blob) indeed reproduces the exact result generating the peaks analogous to the VMD phenomena. For more realistic model calculation, we came up with the LFQM<sup>5</sup> that described the spacelike form factors quite well. In this work, we demonstrated that our model can also be applied to the timelike exclusive processes, analyzing the semileptonic decays of a pseudoscalar meson into another pseudoscalar meson with the same model in Ref.[5]. The form factors  $f_\pm$  are obtained in  $q^+ = 0$  frame and then analytically continued to the timelike region by changing  $q_\perp$  to  $iq_\perp$  in the form factors. The matrix element of the “ $\perp$ ” component of the current  $J^\mu$  is used to obtain the form factor  $f_-$ . Our numerical results are in a good agreement with the available experimental data. This work broadens the standard light-front frame à la Drell-Yan-West to the timelike form factor calculation. The estimation of the zero-mode contribution has also been presented in Ref.[12]. To the extent that the zero-modes have a significant contribution to some physical observables<sup>2</sup>, it seems conceivable that the condensation of zero-modes could lead to the nontrivial realization of chiral symmetry breaking in the light-front quantization approach. The success of our model calculations seems to reveal the effectiveness of light-front degrees of freedom in exclusive processes.

## Acknowledgments

This work was supported by the U.S. Department of Energy(DE-FG-02-96ER4-0947). The North Carolina Supercomputing Center and the National Energy Research Scientific Computing Center are also acknowledged for the grant of computing time allocation. We would like to thank Carl Carlson and Anatoly

Radyushkin for organizing this interesting workshop.

## References

1. S. D. Drell and T. M. Yan, *Phys. Rev. Lett.* **24**, 181 (1970); G. West, *Phys. Rev. Lett.* **24**, 1206 (1970); G. P. Lepage and S. J. Brodsky, *Phys. Rev. D* **22**, 2157 (1980).
2. H.-M. Choi and C.-R. Ji, *Phys. Rev. D* **59**, 034001 (1999).
3. P. L. Chung, F. Coester, and W. N. Polyzou, *Phys. Lett. B* **205**, 545 (1988); W. Jaus, *Phys. Rev. D* **44**, 2851 (1991); F. Cardarelli et al., *Phys. Lett. B* **332**, 1 (1994); *Phys. Rev. D* **53**, 6682 (1996).
4. H.-M. Choi and C.-R. Ji, *Nucl. Phys. A* **618**, 291 (1997); *ibid.* **56**, 6010 (1997).
5. H.-M. Choi and C.-R. Ji, *Phys. Rev. D* **59**, 074015 (1999).
6. M. Sawicki and L. Mankiewicz, *Phys. Rev. D* **37**, 421 (1988); L. Mankiewicz and M. Sawicki, *ibid.* **40**, 3415 (1989).
7. H.-M. Choi and C.-R. Ji, “Exploring the timelike region for the elastic form factor in a scalar field theory”, hep-ph/9906225.
8. J. D. Bjorken and S. D. Drell, *Relativistic Quantum Fields* (McGraw-Hill, New York, 1965), pp. 209-282; S. Gasiorowicz, *Elementary Particle Physics* (Wiley, New York, 1966), pp. 348-362.
9. S. Godfrey and N. Isgur, *Phys. Rev. D* **32**, 189 (1985); N. Isgur, D. Scora, B. Grinstein, and M. B. Wise, *Phys. Rev. D* **39**, 799 (1989); D. Scora and N. Isgur, *Phys. Rev. D* **52**, 2783 (1992).
10. H.-M. Choi and C.-R. Ji, “Light-Front Quark Model Analysis of Exclusive  $0^- \rightarrow 0^-$  Semileptonic Heavy Meson Decays”, to be published in *Phys. Lett. B* [hep-ph/9903496].
11. N.B. Demchuk, I. L. Grach, I. M. Narodetskii, and S. Simula, *Phys. At. Nuclei* **59**, 2152 (1996); H.-Y. Cheng, C.-Y. Cheng, and C.-W. Hwang, *Phys. Rev. D* **55**, 1559 (1997).
12. H.-M. Choi and C.-R. Ji, *Phys. Rev. D* **58**, 071901 (1998).
13. Particle Data Group, C. Caso et al., *Eur. Phys. J. C* **3**, 1 (1998).